RESEARCH ARTICLE

Feeding a low-protein diet exacerbates the susceptibility to *Citrobacter rodentium* and dextran sulfate sodium-induced intestinal injury in mice

Mehakpreet K. Thind[1,2☯], Mary Flanagan[2,3☯], Sanne de Wit[4], Aida Glembocki[5,6,7], Jiali Pan[1], Celine Cuinat[1], Sharon Leung[8], Shamsun Nahar Shaima[1,2], Hamza Sghayare[2], Kinza Usmani[2], Mishaal Munawar[8,9], Peter Kim[8,9], Elena M. Comelli[1,10], Amber Farooqui[2], Celine Bourdon[2], Robert H. J. Bandsma[1,2,3]*

1 Department of Nutritional Sciences, Faculty of Medicine, University of Toronto, Toronto, Ontario, Canada, **2** Translational Medicine Program, The Hospital for Sick Children, Toronto, Ontario, Canada, **3** Division of Gastroenterology, Hepatology and Nutrition, The Hospital for Sick Children, Toronto, Ontario, Canada, **4** Department of Cardiology, University Medical Center Groningen, Groningen, Netherlands, **5** Department of Pathology and Laboratory Medicine, Western University and London Health Sciences Centre, London, Ontario, Canada, **6** Child Health Evaluative Sciences, The Hospital for Sick Children, Peter Gilgan Centre for Research and Learning, Toronto, Ontario, Canada, **7** Institute of Health Policy, Management and Evaluation, University of Toronto, Toronto, Canada, **8** Cell Biology Program, The Hospital for Sick Children, Toronto, Ontario, Canada, **9** Department of Biochemistry, Faculty of Medicine, University of Toronto, Toronto, Ontario, Canada, **10** Centre for Child Nutrition and Health, Faculty of Medicine, University of Toronto, Toronto, Ontario, Canada

☯ These authors contributed equally to this work.
* robert.bandsma@sickkids.ca

Check for updates

OPEN ACCESS

Citation: Thind MK, Flanagan M, de Wit S, Glembocki A, Pan J, Cuinat C, et al. (2026) Feeding a low-protein diet exacerbates the susceptibility to Citrobacter rodentium and dextran sulfate sodium-induced intestinal injury in mice. PLoS One 21(10): e0335322. https://doi.org/10.1371/journal.pone.0335322

Editor: Maria Leonor S Oliveira, Instituto Butantan, BRAZIL

Received: October 9, 2025

Accepted: August 17, 2026

Published: October 7, 2026

Peer Review History: PLOS recognizes the benefits of transparency in the peer review process; therefore, we enable the publication of all of the content of peer review and author responses alongside final, published articles. The editorial history of this article is available here: https://doi.org/10.1371/journal.pone.0335322

Copyright: © 2026 Thind et al. This is an open access article distributed under the terms of the Creative Commons Attribution License, which permits unrestricted use, distribution,

Abstract

Globally, almost half of all early childhood deaths are linked to severe undernutrition, herein referred to as severe malnutrition. Mortality in severely malnourished children is often attributed to common infectious diseases, including enteric infections. It has been proposed that impaired intestinal barrier function contributes to mortality, but direct evidence is limited and thus there exists a need to develop improved preclinical models to test these and other mechanistic hypotheses. In this study, we aimed to describe differences in response to enteric inflammation and infection in the colon of malnourished mice compared to well-nourished littermates. C57Bl/6 male weanlings were fed isocaloric diets, either a low 1% protein diet (LPD) or a control 18% protein diet (CPD) for 2-weeks either in combination with oral administration of dextran sodium sulfate (DSS), or *Citrobacter rodentium* (*C. rodentium)*. LPD-fed mice were more susceptible to DSS or *C. rodentium* as evidenced by increased clinical severity scores, and reaching their humane endpoints. LPD-fed mice also showed more signs of colonic dysfunction with reduced levels of tight junction proteins, higher colonic pathogen load, and increased systemic inflammation and bacterial spread. Taken together, these observations show that malnourished animals have increased susceptibility to intestinal dysfunction caused by either chemical exposure or infection.

and reproduction in any medium, provided the original author and source are credited.

Data availability statement: All relevant data are within the manuscript and its Supporting information files.

Funding: R.J.B - Bill & Melinda Gates Foundation (OPP1185057) and the Canadian Institutes of Health Research (CIHR156307) The funders played no role in the study design, data collection and analysis, decision to publish, or preparation of the manuscript.

Competing interests: Amber Farooqui is currently employed by Omega Laboratories Inc, a clinical diagnostic laboratory. This does not alter our adherence to PLOS ONE policies on sharing data and materials. The other authors declare no competing interests.

These novel preclinical models can be used to further elucidate the processes involved in enteric dysfunction in malnutrition and to test therapies to improve intestinal repair and outcomes.

Introduction

Severe malnutrition (SM), herein referring to early childhood undernutrition, is associated with high morbidity and mortality of children under 5 years of age living in low-resource settings [1]. SM encompasses two major forms of malnutrition, severe wasting (most common, also known as marasmus) or nutritional edema (also known as kwashiorkor), and SM is associated with immunodeficiency and environmental enteropathy (EE) in children [2–4]. EE is characterized by high exposure to environmental microbes and linked to villous atrophy, intestinal inflammation and signs of epithelial barrier dysfunction [5–8], which is strongly related to poor clinical outcomes [7–11]. In fact, in children with SM and EE, exposure to common pathogens can become life-threatening [2,4,8,10–15]. Gram-negative bacteria commonly found in blood of acutely ill children with SM and associated with diarrhea include enteric pathogens such as *Salmonella typhimurium*, *Shigella spp,* enteropathogenic *Escherichia coli* (EPEC), and *Klebsiella pneumoniae* [16–19]. This suggests that children with SM are more vulnerable to bacterial translocation across the intestinal lumen leading to sepsis. This could be more likely to occur in the large intestine where bacterial density is the highest. In addition, there exists a positive association between diarrhea and mortality in children with SM [17,20]. Despite following established treatment regimens, including the widespread use of broad-spectrum antibiotics, the in-patient and post-discharge mortality rate of children with SM remains high [1] and therefore should be a prioritized area of research.

Pre-clinical models can be used to elucidate the pathophysiological processes and identify treatment approaches that could improve intestinal dysfunction associated with SM [21–24]. This would otherwise not be possible as non-invasive methods in this clinical setting are limited and invasive methods such as endoscopy and colonoscopy pose a risk to this highly vulnerable population. Several animal models have been developed to study malnutrition, typically wasting, and intestinal changes [5,6,15,22,23,25–28]. For example, mice fed a moderately low-protein diet (7%) developed enteric dysfunction if also exposed to specific bacteria (i.e., Bacteroidales and *E. coli* strains) [15]. Similarly, post-weaning mice fed a moderately-low protein diet (5.8%) developed intestinal dysfunction after receiving an additional gastrointestinal insult (indomethacin or lipopolysaccharide (LPS)) [29]. In these models, wasting was not severe and, while intestinal dysfunction was induced after the additional insult, the mice did not develop severe infection.

More recently, a study showed that feeding a corn-based diet with nutritional deficiencies in protein, fat, minerals and vitamins, as commonly consumed in resource poor settings, to weanling mice for 28-days was sufficient to induce anthropometric deficits, dysbiosis, enteric dysfunction and immune alterations [22]. Similarly, 14-days

of severe protein deficiency (1%) alone has been shown to induce highly significant linear growth impairment and wasting as well as enteric dysfunction in mice [5,6,25].

However, the susceptibility to enteric infection and inflammation in severely wasted mice, particularly in the colon, remains poorly studied. Furthermore, whether malnutrition exacerbates bacterial translocation across the intestinal barrier in the context of enteric infection has not been demonstrated directly. Dextran sodium sulfate (DSS), a chemical insult, is well-known to induce acute colitis characterized by bloody diarrhea, mucosal ulcerations and innate immune cell infiltration through its toxic effects to gut epithelial cells that impacts the integrity of the mucosal barrier, and causes subsequent colonic inflammation [30]. *Citrobacter rodentium* (*C. rodentium)* is an extracellular, gram-negative enteric pathogen that is commonly used to model human intestinal diseases, such as EPEC and enterohemorrhagic *Escherichia coli* (EHEC) infections, in mice [31,32]. It establishes colonization by adhering and forming attaching-and-effacing lesions on the colonic gut epithelium inducing an infection response similar to EPEC and EHEC [31], including crypt hyperplasia. Colonic crypt hyperplasia involves the proliferation of transit amplifying cells and is a typical tissue response to *C. rodentium* colonization [31,33–35]. This current study aimed to describe novel mouse models of severe wasting and large intestinal infection and inflammation and assess the impact on intestinal epithelial barrier function.

Materials and methods

Animals

All mouse experiments were approved and conducted in strict accordance with the Animal Care and Use Committee guidelines (protocol number: 1000058060) at Lab Animal Services (LAS) Facility of SickKids, Toronto. Reporting follows ARRIVE guidelines. C57Bl/6J mice sourced from The Jackson Laboratory (Bar Harbor, Maine USA) were bred and maintained as a specific pathogen free colony. Male weanlings (21 days old) were weight-matched and randomized to one of two diet groups. For 14 days, mice received either: (1) a control 18% protein diet (CPD; TD: 180483), or (2) a 1% low-protein diet (LPD; TD: 180481) made by Envigo Teklad Diets (Madison, WI). The diets were isocaloric where the decrease in casein was compensated with an increase in corn starch (diet composition detailed in S1 Table). All animals were group housed at 22°C, following a 12-h light-dark cycle and had *ad libitum* access to food and water. Reseaches were unblinded to the treatment groups.

DSS-induced colitis

To induce colitis, mice fed either CPD or LPD were administrated dextran sulfate sodium (DSS, molecular weight 40 kDa; ThermoFisher, Massachusetts, USA) in drinking water as follows: 1% DSS for 3 consecutive days or 2% DSS for 5 consecutive days starting on day 7. After dosing, animals were returned to normal drinking water. Body weight, and food/water consumption was recorded daily. To minimize animal suffering, clinical severity scores [33,36] were determined daily by trained staff for each mice post DSS administration that included clinical signs such as hunched posture, inactivity, ruffled fur, diarrhoea and bloody stools (S2 Table). A score of 35 or higher was considered the humane endpoint, and animals were removed from the study early and euthanized immediately if they reached humane endpoints prior to completing the study. All other animals were euthanized on the last day of the experiment (study day 14). The results from the mice excluded early were used for the survival curve graphs only.

Bacterial preparation, dosing and gavage

Wildtype *Citrobacter rodentium* strain DBS100 bacteria was grown to log phase in Luria-Bertani (LB) broth with streptomycin at 37°C for 2hr to an optical density (OD) at 600 nm of 1 ($3.7X10^8$ colony-forming unit (CFU)/mL). CPD and LPD-fed mice were infected on day 7 of the experimental period through oral gavage with either 100 µL of inoculum containing a total of 10^7 CFU bacteria in PBS or of sterile PBS and were sacrificed 7 days later. To confirm dosage, left over inoculum

were serially diluted in PBS, plated on LB agar and grown aerobically at 37 °C for 24 h to verify administered CFU. Monitoring of animals was performed similarly as for mice exposed to DSS-colitis.

Euthanasia and tissue collection

After the 14 day experimental period, mice were put under anesthesia with isoflurane and euthanized by cervical dislocation. Liver, spleen and colon were collected for the *Citrobacter rodentium* infected mice. Liver and spleen were weighed, and tail and colon length were measured.

Quantification of *C. rodentium* in stool

DNA was extracted from feces collected at 4- and 7-days post-infection using the E.Z.N.A™ Stool DNA Isolation Kit (Omega Bio-Tek, Doraville, GA, USA), as per manufacturer's instructions. DNA concentration was quantified using a Nanodrop (Thermo Scientific) and reactions contained advanced SYBR green qPCR mastermix (Wisent), 50 nM of forward primer, 300 nM of reverse primer and 50 ng of DNA in a final volume of 10 µl. Reactions were performed in triplicates in 384-well plates using CFX384 Touch Real-Time PCR Detection System (Bio-Rad). We used a primer set designed to target the C. *rodentium* specific espB gene (espB-F: 5′-ATGCCGCAGATGAGACAGTTG-3′ and espB-R: 5′-CGTCAGC AGCCTTTTCAGCTA-3′, Invitrogen) which were previously determined to show sensitive quantification of *C. rodentium* [37]. The cycling conditions were: incubation at 95°C for 10 minutes, followed by 40 cycles of 15 seconds of denaturation at 95°C, and 1 minute of annealing/extension at 60°C. For absolute quantification of bacterial loads, a standard curve was constructed using 10-fold serial dilutions of DNA extracted from a known number of *C. rodentium* cells, counted in triplicates using a hemacytometer.

Detection of *C. rodentium* in tissue

To evaluate bacterial dissemination into distant tissues, liver and spleen samples were homogenized in 1 ml of sterile PBS, and serial dilutions were plated on LB agar plates with streptomycin and incubated aerobically at 37°C overnight. The number of colonies were counted and plotted as a CFU count/gram tissue.

Histology

Colons were fixed in 10% formalin and were processed for paraffin-wax embedding using an automated processor. Tissue blocks were cut at 5 µm thickness, and sections were stained with hematoxylin and eosin (H&E). Digital light microscopic images were acquired using Aperio AT2 (Leica Biosystems, Ontario, Canada). A blinded experienced pathologist (A.G.) assessed the severity of colonic inflammation according to an established scoring scheme [38]. Using the ImageJ Software [39], the length of at least 30 crypts were measured per mouse and a mean per mouse was calculated and analysed. Immunofluorescence and data analysis was performed for Ki67 as described previously [5]. Imaging of Ki67 was performed on a Zeiss LSM980 with Airyscan 2 confocal microscope, using a 63x/1.4 NA Plan-APOCRAMAT oil immersion objective. Briefly, the average of four intestinal crypts for each sample was counted to calculate the mean for Ki67-positive cells per crypt.

Serum collection and ELISA for IL-22

Whole blood collected through cardiac puncture was allowed to clot at room temperature for 30 min. Samples were then centrifuged at 15,000 r.p.m., 4°C for 20 min. Supernatants were transferred to 1.5 mL Eppendorf tubes and stored at −80 °C for downstream analysis. To quantify IL-22, serum was collected as described and an IL-22 ELISA (IL-22, Cat# ab223857) was performed according to the manufacturers' instructions. IL-22 concentration was measured at 450 nm with a plate reader.

Western blotting

Colonic tissues were sonicated on ice in tissue lysis buffer (Thermo Scientific) with a cocktail of protease inhibitors (Sigma). Protein concentration was measured using BCA Protein Assay Kit (Thermo Scientific) as per manufacturer's protocol. 20 μg of protein was electrophoresed through layered gels made in-house (polyacrylamide concentration: stacking gel, 4%; top resolving gel 12% and bottom resolving gel 16%). Trans-Blot Turbo Transfer System (Bio-Rad) was used for semi-dry transfer (14 min) onto a polyvinylidene fluoride (PVDF) membrane (Millipore) with 0.45 μm pore size. Membranes were blocked for 1 h at room-temperature in TBS-Tween 0.1% containing 3% BSA. Membranes were incubated in primary antibody overnight at 4 °C, followed by secondary HRP-conjugated antibody incubation for 2 hours at room temperature. Antibody concentrations used and catalogue numbers are detailed in S3 Table. Proteins were visualized using a Pierce enhanced chemiluminescence (ECL) kit (Invitrogen, USA), images were captured using the Odyssey Imaging System (LI-COR) and analyzed using Image Studio Lite v.5.2.5 (LI-COR). After quantification, Restore™ Western Blot Stripping Buffer (Thermo Fisher Scientific, USA) was used to remove primary and secondary antibodies, allowing the same membrane to be reprobed with a different antibody. Uncropped raw blots are provided as S3 Fig.

Statistical analysis

Statistical analysis was done using Prism 9 software (GraphPad Software, San Diego, California USA). Data are represented as the mean ± SD. As detailed in figure legends, statistical comparisons and continuous normally distributed variables were evaluated with either unpaired, two-tailed student's t-test (for two groups) or one-way ANOVA (for multiple groups) followed by Tukey's multiple comparisons test. For ordinal, non-normal or categorical data, non-parametric unpaired, two-tailed Mann-Whitney test, and Fisher's exact test was applied. Linear mixed-effect model was applied for the clinical severity score data. Kaplan-Meier survival was analyzed by Mantel-Cox Logrank test. To assess group differences in repeated measures, two-way ANOVA followed by Tukey's multiple comparisons test was used. $P < 0.05$ was considered statistically significant.

Results

Low-protein diet feeding exacerbates the effect of DSS-treatment in weaning mice

First, we used DSS to induce acute colitis in mice [30] fed either a low- or control- protein diet to study differences in disease burden. Weanling C57Bl/6 male mice were randomised into two groups fed either the low 1% protein diet (LPD) or the 18% control protein diet (CPD) for 14 days. On day 7, groups were provided water containing either 1% or 2% DSS for either 3 or 5 days, respectively (Figs 1a; S1a). As previously demonstrated [5,6,25], CPD-fed mice gained approximately 40% of their body weight over the 14 days, whereas LPD-fed mice lost approximately 20% of their body weight (Figs 1b; S1b). The malnourished mice showed minimal clinical features and had higher clinical severity scores largely due to weight loss. When exposed to 1% or 2% DSS, the LPD-fed mice lost significantly more weight compared to controls (Figs 1b; S1b). Furthermore, LPD-fed mice exposed to DSS also exhibited more clinical symptoms especially relating to diarrhea, bloody stools and reduced mobility. Thus, the DSS-exposed LPD-fed mice had higher clinical severity scores (S1 Table; Figs 1c; S1c). 60% of these DSS-exposed malnourished mice died or reached pre-defined humane endpoints (Figs 1d; S1d), while all DSS-exposed controls survived. Overall, these findings highlight that LPD feeding increases the host susceptibility to DSS-induced colitis.

Susceptibility to infection with *C.rodentium* is increased in low-protein diet fed mice

Next, we explored whether mice fed a low-protein diet were more susceptible to intestinal infection by *C.rodentium*, a gram-negative pathogen. To do this, we inoculated the mice by oral gavage with 10^7 colony forming units (CFU), a lower infective dose compared to the more typically used 10^8–10^9 CFU (Fig 2a). This lower dose reduces the likelihood of early mortality or reaching humane endpoints prematurely in young mice [40,41]. As expected [5,6,15,25,42], LPD-fed mice inoculated with *C. rodentium* had shorter tail length (which represents stunted growth) (S2a Fig). Their colon length was also

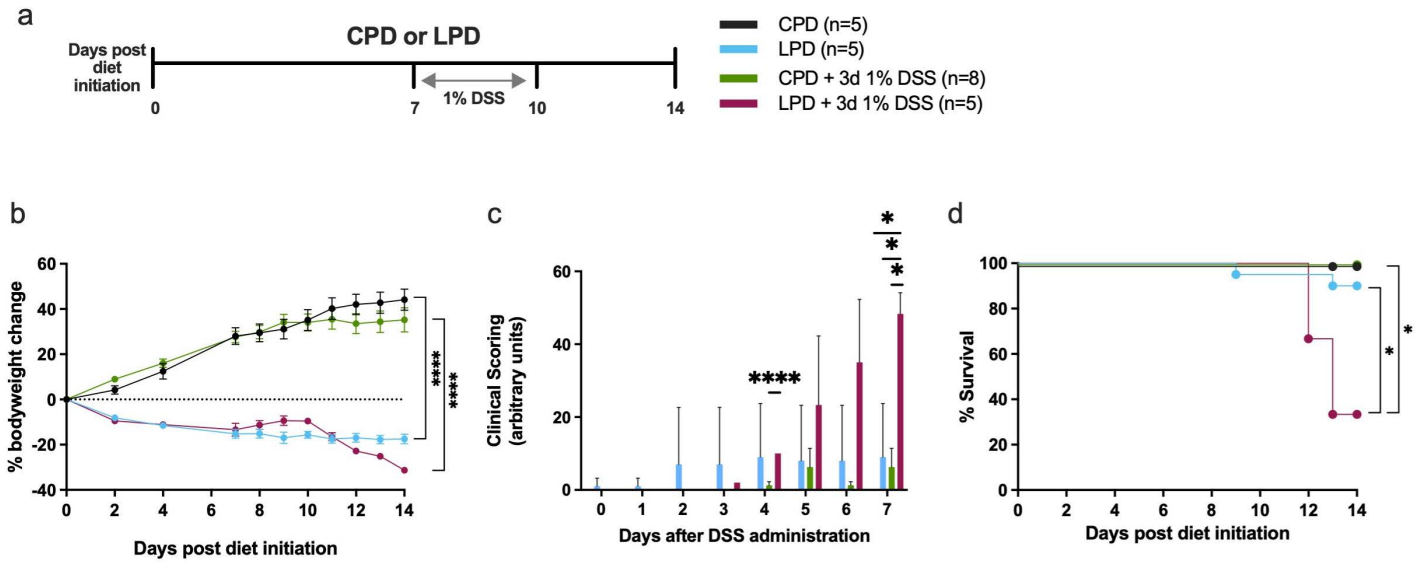


Fig 1. Mice fed a low-protein diet are more susceptible to DSS-induced colonic inflammation. (a) Experimental design of the DSS-induced colitis; weanling C57Bl/6 mice fed control (CPD) or the low-protein diet (LPD) were given either 1% DSS dissolved in drinking water for 3 days or DSS-free drinking water. (b) Percent bodyweight change from day 0 and (c) Clinical Severity Scoring (CSS) over time. CSS is a measurement of hunched posture, ruffled fur, immobility, weight loss, diarrhea and bloody stools [33,36]. (d) Survival of CPD and LPD- fed mice. Results are expressed as means ± SD and *p < 0.05; ****p < 0.0001, as determined by (b) two-way ANOVA, (c) linear mixed-effect analysis and (d) two-sided log-rank (Mantel-Cox).

https://doi.org/10.1371/journal.pone.0335322.g001

shorter (S2b Fig; 5.58 ± 0.58 vs. 4.47 ± 0.45, p < 0.0001) and their ratio of colon over tail length was also significantly lower compared to CPD-fed mice post-infection (S2c Fig; 0.77 ± 0.09 vs. 0.71 ± 0.06, p < 0.0001). After infection, the LPD-fed mice had, at day 4 and 7, more *C. rodentium* in their stool compared with CPD mice (Figs 2b; S2d). This suggests that malnourished mice experience higher pathogen colonization and/or have a reduced ability to clear pathogenic bacteria. Similarly, systemic levels of IL-22, a pro-inflammatory cytokine, were higher in LPD-fed mice 7 days post- *C. rodentium* infection (Fig 2c). With infection, 25% of LPD-fed mice reached the humane endpoint, mostly due to more than 25% weight loss (Fig 2d-e). Reaching their humane endpoint prevented us from studying mice for a longer period post-infection. As previously reported [43,44], no change in body weight was observed in CPD-fed mice after *C. rodentium* infection.

Crypt hyperplasia caused by *C. rodentium* is blunted in low-protein diet fed mice

We next determined whether the higher bacterial load and a trend towards lower survival of LPD mice was associated with changes in hyperplasia of colonic crypts that is typically observed in response to *C. rodentium*. Without infection, LPD-fed mice had a shorter crypt length compared to controls (Fig 3a-b). This is in line with previously published data [5,6]. Also, the colons of LPD-fed mice did not show differences in histological signs of inflammation (Fig 3c). CPD-fed mice infected with *C. rodentium* exhibited a trend towards increased colonic inflammation, without significant alterations in crypt length (Fig 3a-c). This response is characteristic of *C. rodentium*-induced intestinal inflammation and is thought to limit systemic pathogen dissemination while promoting epithelial repair and regeneration [31]. In contrast, infected LPD-fed mice showed a lack of crypt hyperplasia (Fig 3a-b), and insignificant colonic inflammation compared to LPD-alone and infected CPD-fed mice (Fig 3c). In line with this, the expression of Ki67, a marker of cell proliferation, increased in the colonic crypts of CPD-fed mice but its expression was unaltered in the colonic crypts of LPD-fed mice post-infection (Fig 4). These findings suggest that malnourished mice have a reduced ability to initiate a protective colonic response to *C. rodentium,* potentially leading to poor pathogen clearance.

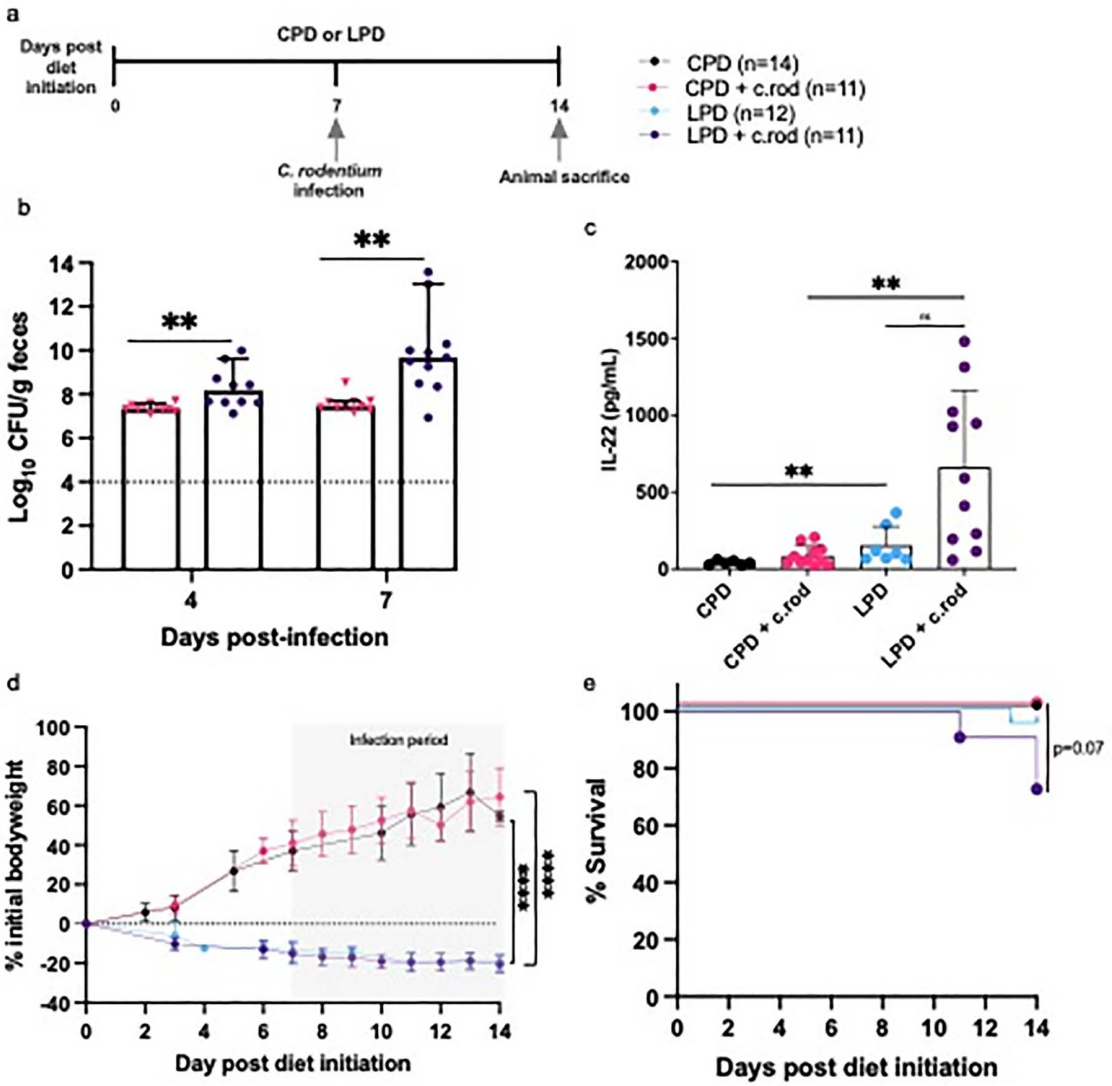


Fig 2. Mice fed a low-protein diet are more susceptible to *Citrobacter rodentium* infection. (a) Experimental design of *Citrobacter rodentium* (*C. rodentium*) infection; weanling C57Bl/6 mice fed control (CPD) or the low-protein diet (LPD) were inoculated by gavage with $1X10^7$ colony forming unit (CFU) of *C. rodentium*. (b) qPCR quantification of *C. rodentium* in stool at day 4 and 7 post-infection in CPD and LPD mice. Dotted line represents the limit of detection for *C. rodentium*, as previously published [37,45]. (c) Mice were sacrificed on day 7 post-infection and IL-22 concentration was measured by ELISA in serum. (d) Change in body weight and (e) survival of CPD and LPD mice. Results are expressed as means ± SD and **p < 0.01; ***p < 0.001; ****p < 0.0001, as determined by (b) two-way ANOVA, unpaired two-tailed Mann-Whitney test, and Fisher's exact test, (c) one-way ANOVA with Tukey's multiple comparisons test and unpaired two tailed t-test analysis, (d) two-way ANOVA and mixed-effect analysis, and (e) two-sided log-rank (Mantel-Cox).

https://doi.org/10.1371/journal.pone.0335322.g002

Increased susceptibility to *C. rodentium* is associated with loss of colonic barrier integrity in low protein diet-fed mice

To assess whether *C. rodentium* infection and invasiveness was associated with loss in colonic barrier integrity, we measured the tight junction proteins CLD-3 and occludin. In uninfected LPD-fed mice, changes in CLD-3 were not observed (Fig 5a-b), but occludin levels were higher compared to controls (Fig 5a,c). With *C. rodentium* infection, tight junction proteins differed between diet groups, where the colonic expression of CLD-3 decreased in LPD-fed mice compared to

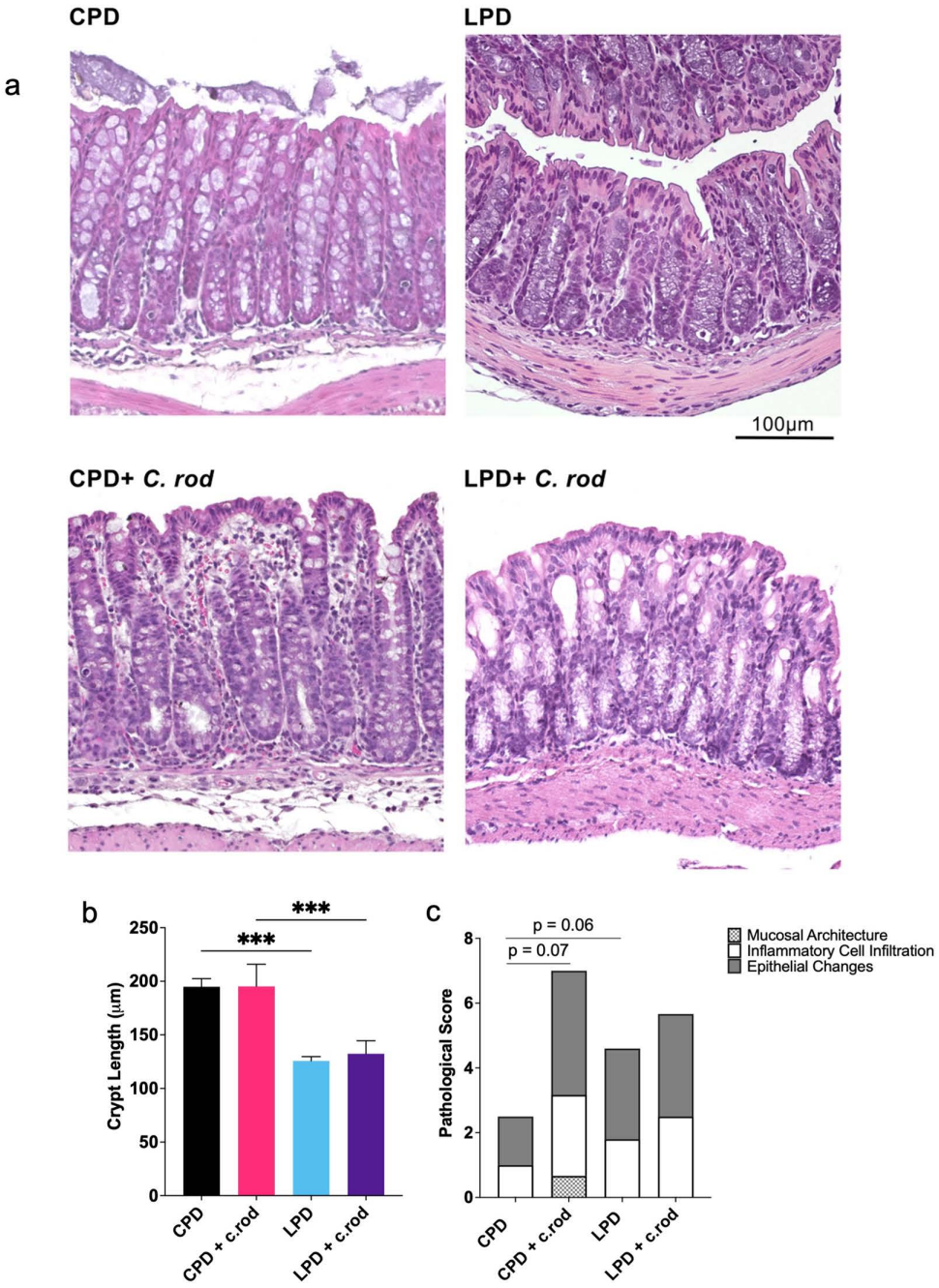


Fig 3. Assessment of colonic inflammation due to *Citrobacter rodentium* infection. (a) Representative images of colon (H&E, 20x). Scale bar, 100 µm. (b) Quantification of crypt hyperplasia calculated from the mean length of 30 crypts per animal (n ≥ 5/group) and (c) and cumulative pathology score on day 7 post infection (n ≥ 5/group). Results are expressed as means ± SD; *p < 0.05; **p < 0.01; ****p < 0.0001, as determined by (b) two-way ANOVA and (c) one-way ANOVA with Tukey's multiple comparisons test and unpaired two tailed t-test analysis.

https://doi.org/10.1371/journal.pone.0335322.g003

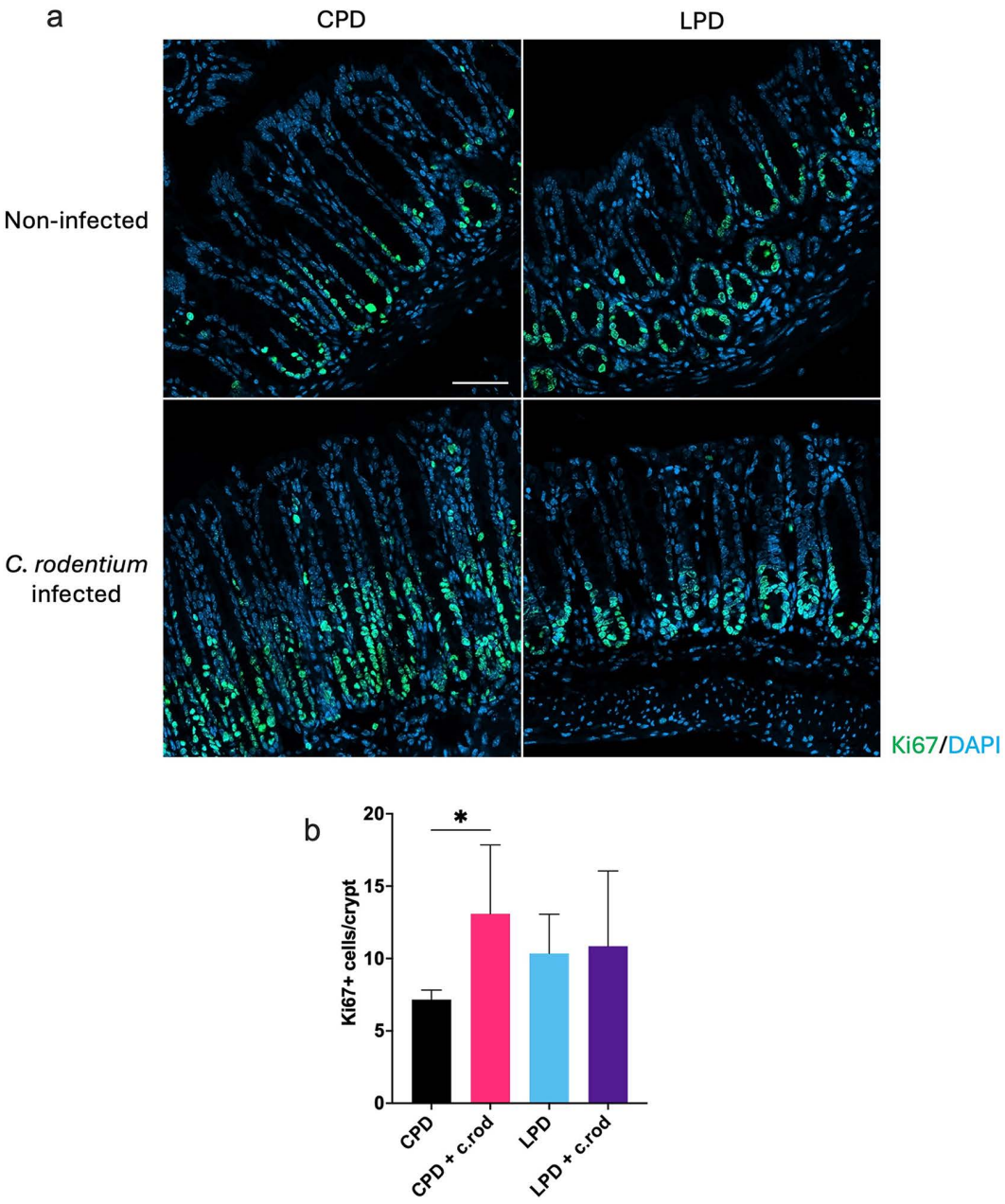


Fig 4. Expression of Ki67, a proliferation marker, in colon of *Citrobacter rodentium* infected mice. (a) Representative confocal microscopy images (63x) of proliferation marker Ki67 (green) in the colon with DAPI counterstaining of nuclei in blue. Scale bar, 50 μm. (b) Quantification of Ki67 + cells per crypt in the colon (n ≥ 3 mice, 4 crypts per mouse). Results are expressed as means ± SD; *p < 0.05, as determined by (b) one-way ANOVA with Tukey's multiple comparisons test and unpaired two tailed t-test analysis.

https://doi.org/10.1371/journal.pone.0335322.g004

controls (Fig 5a-b). However, occludin was similarly elevated in all conditions compared to CPD mice (Fig 5a, c). Given the impact of *C. rodentium* on barrier integrity in this study, we evaluated for evidence of bacterial translocation in the spleen and liver, tissues known to be first exposed to bacteria entering the circulation due to breaches in intestinal barrier [46–48]. We found significantly higher *C. rodentium* bacterial counts in liver homogenates from LPD-fed mice, while a

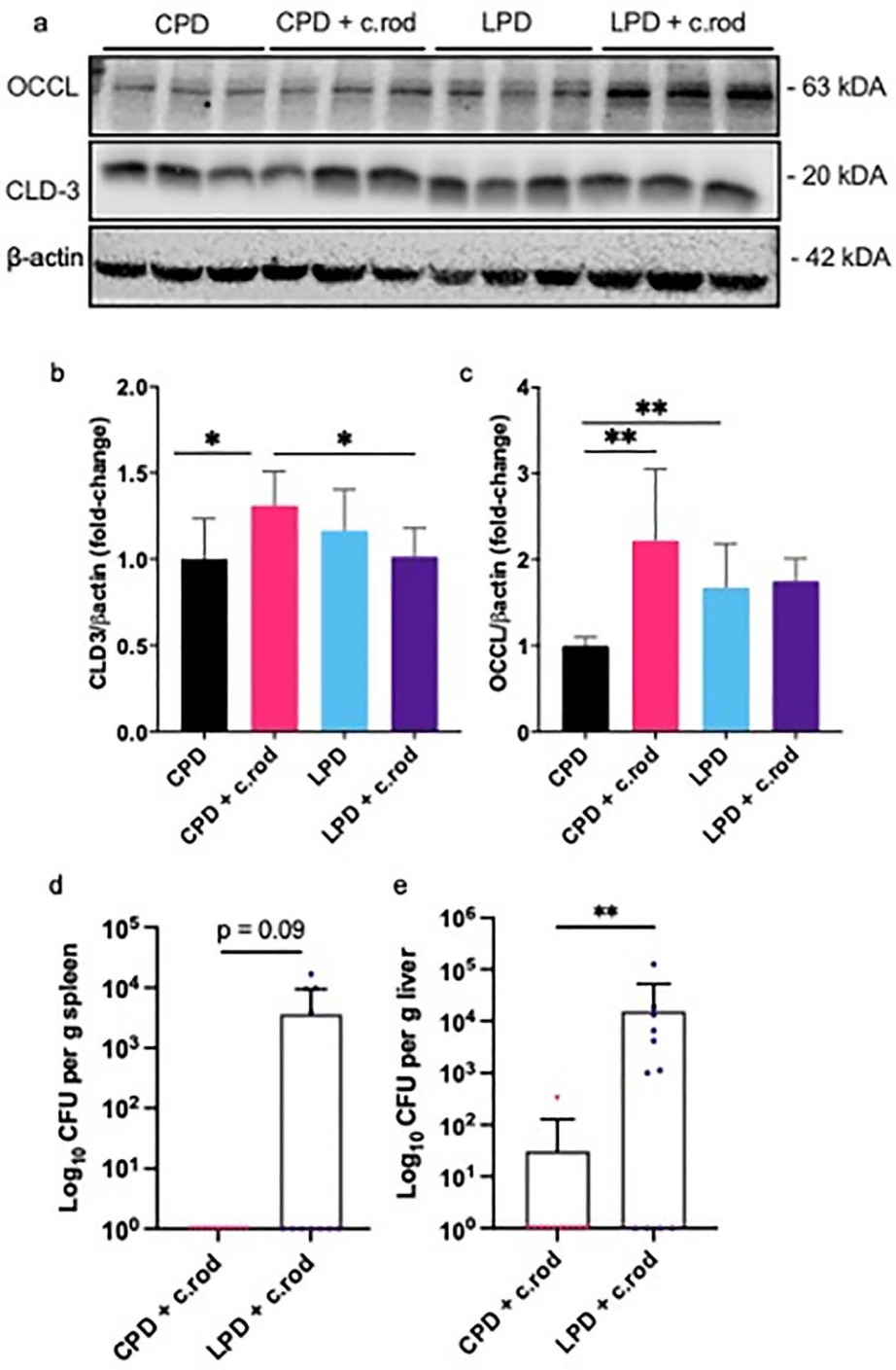


Fig 5. *Citrobacter rodentium* infection alters colonic structural integrity and promotes systemic bacterial translocation in malnourished mice. (a) Representative cropped western blot membranes probed for claudin-3 (CLD-3), and Occludin (OCCL) and β-actin in colonic tissue of uninfected and infected CPD and LPD-fed mice. Full uncropped blots are presented in S3 Fig. Quantification of (b) CLD-3, and (c) OCCL normalized to β-actin in CPD colonic tissue was calculated (n = 6/group). Bacterial burden in the (d) spleen, and (e) liver expressed as CFU per gram of tissue. Results are presented as means ± SD; *p < 0.05; **p < 0.01, as determined by (b-c) one-way ANOVA with Tukey's multiple comparisons test and unpaired two tailed t-test analysis, and (d-e) unpaired two tailed Mann-Whitney test and Fisher's exact test.

https://doi.org/10.1371/journal.pone.0335322.g005

trend towards higher bacterial counts was also observed in the spleen, consistent with increased translocation (Fig 5d-e). Together, these findings demonstrate that LPD-fed mice show an increased susceptibility to a low infectious dose of *C. rodentium* which is associated with reduced markers of colonic barrier integrity and with higher dissemination of bacteria within the host.

Discussion

We developed two complementary novel "double insult" models of malnutrition with colonic infection/inflammation and demonstrated that mice fed a low-protein diet exhibited decreased survival and increased colonic dysfunction when exposed to chemically induced intestinal inflammation by DSS or a low dose infection by *C. rodentium*. These pre-clinical models provide valuable tools to study the pathophysiological processes underlying increased susceptibility to intestinal disease associated with malnutrition. By establishing these models, we aimed to facilitate the testing and development of novel therapeutic approaches that could improve disease response and/or accelerate tissue repair of the colon in malnourished hosts.

To our knowledge, we are the first to show that mice fed a low-protein diet exhibit an altered colonic response to exposure of DSS or *C. rodentium* compared to mice fed a regular diet. Our findings are complimentary to previous observations in the small intestine, where dietary insults alone [5,6,22] or in combination with specific bacteria [15,21,29,49] have been shown to recapitulate elements of enteropathy associated with malnutrition [22,50–53]. Mice fed with a moderately low protein diet (7%) showed villous blunting, reduced barrier function (reduction of CLD4 expression) and intestinal permeability, assessed by higher fluorescein isothiocyanate (FITC)-labelled dextran in the serum. Here, dissemination of bacteria and systemic inflammation occurred only after exposure to a mixture of Bacteroidales and *E. coli* [15]. Similarly, mice fed a moderately low protein (5.8%) with repeated oral doses of indomethacin also showed impaired gut barrier function (higher FITC in serum) [29].

We chose DSS and *C. rodentium* to mimic symptoms of diarrhea described in children [16,54,55]. More specifically, *Shigella*, heat-stable enterotoxin-producing *Escherichia coli* (ST-ETEC), *Campylobacter*, and typical enteropathogenic *E coli* were recently shown to be the leading causes of diarrhea [56,57] and these bacterial pathogens were associated with linear growth faltering [56] and death [57]. C*. rodentium* is a murine mucosal pathogen that shares pathogenic mechanisms with human EPEC and EHEC infections and has been widely used to study the pathogenesis of these two clinically important human gastrointestinal pathogens [31,58]. The DSS-induced inflammatory insult is also a commonly used pre-clinical model of colitis and IBD, and this model is relevant to malnutrition since it presents with several overlapping features, such as intestinal inflammation, poor intestinal absorption, and disrupted barrier function [59,60]. Despite using lower doses of DSS and *C. rodentium*, we found the models to be robust and reproducible.

Colonic hyperplasia in *C. rodentium* infection has been attributed to hyperproliferation of the transit amplifying cells and $LGR5^+$ cells via activation of the Wnt/β-catenin signaling pathway [61]. This increases cell turnover, facilitating shedding of infected cells into the lumen, promoting pathogen clearance, and restoring intestinal homeostasis in a self-limiting manner [31]. In this study, malnourished mice exhibited a blunted crypt hyperplasia response at 1-week post- infection with C. *rodentium*, likely due to a reduced proliferative capacity as demonstrated by the reduced Ki67-positive colonic epithelial cells in mice fed a low-protein diet (Fig 4). Interestingly, unlike the jejunum and ileum of non-infected malnourished mice where a significant decrease in Ki67 expression was reported [5], there was no difference between non-infected CPD and LPD mice in the colon in our study. Overall, impaired cellular turnover and shedding could potentially be related to the increased intestinal colonization and systemic dissemination in malnourished hosts observed in this study.

It is hypothesized that malnutrition is associated with an increased susceptibility to enteric infection and inflammation due to underlying enteric dysfunction and immune defects that increases susceptibility to systemic bacterial burden and inflammation, and mortality. We report for the first time that mice fed a LPD exhibit enhanced systemic translocation of pathogens that typically cause colonic infection. Scarce data existed prior to this study in support of increased risks of

bacterial translocation in malnourished conditions. Mice fed a 3% protein diet deficient in calories, zinc and iron for 28 days showed exaggerated translocation of intestinal microbiota and their products, i.e., LPS, after exposure to intradermal systemic infection, compared to control mice [62]. Another dietary model to induce malnutrition (7% protein and 5% fat) led to higher bacterial burdens of S. Typhimurium in the small intestine, as well as increased colonization in the liver and spleen [15]. Additionally, children in Zambia, with SM and persistent diarrhea were found to have higher damage in the small intestine—reduced epithelial surface, histological lesions and disruptions of claudin-4 and E-cadherin—and subsequent higher levels of circulating LPS, which was used as a marker of bacterial translocation [7]. A higher blood concentration of 16S rRNA gene copy numbers was also observed among children with complicated SM in Uganda due to impaired gut function [63].

Epithelial barrier integrity is a dynamic process that relies on several tight junction proteins to regulate paracellular permeability and protect against pathogens [64–66]. When exposed to *C. rodentium,* well-nourished mice tended to increase CLD3 and occludin, whereas this cohesive increase in tight junction proteins was blunted in malnourished mice. Brown et al. also reported reductions in these tight junction proteins in mice fed a moderately low-protein diet and exposed to a mixture of Bacteroidales and E. Coli [15]. Altered expression of claudins and occludins were also implicated in poor response to EPEC infections in preclinical models of inflammatory bowel disease [15,34,62,67,68]. Therefore, structural perturbations in tight junction proteins during *C. rodentium* infection [44] could also contribute to the systemic spread of bacteria to the spleen and liver in severely malnourished hosts.

The increased susceptibility of malnourished mice may also be attributed to poor immune responses [69], as has been demonstrated in recent clinical studies [14,35]. Early childhood malnutrition impairs both innate and adaptive immunity reducing the capacity to clear pathogens, despite high systemic and intestinal inflammation [2,4,16,70]. In particular, neutrophils—key first responders to pathogens—show impaired antimicrobial responses in malnutrition despite having elevated numbers [4,13,69,71]. Neutrophils are also major producers of IL-22, a cytokine that regulates crypt hyperplasia [72] and secretion of antimicrobial proteins in response to early C. *rodentium* infection to maintain the epithelial barrier function [73,74]. In DSS-induced intestinal damage, IL-22 modulates repair of colonic epithelium [75], where exogenous supplementation of IL-22 improves response. However, persistent elevations in IL-22 levels, as we observed in this study, are also implicated in chronic inflammatory conditions through sustained immune responses and inflammation [76], and could be a driver of the exacerbated pathology observed in this study in the LPD-fed mice.

This study had several limitations. The model diet used in this study aimed to mimic the carbohydrate-rich and protein-poor staple foods, such as cereals and starches, suboptimal in essential amino acids, that malnourished children in low-income countries are generally exposed to. However, this study did not determine if there is a specific contribution of a difference in starch on our phenotype. Additionally, the incidence of bacterial translocation may have been underestimated since translocation was only studied at a single time point post-infection. The experimental timeline was another major limitation. A 7-day timeline post-infection is insufficient to observe the full evolution of epithelial hyperplasia, which typically peaks around 10–12 days post-infection in adult mice. Multiple pathogens are commonly detected in ill children with severe malnutrition [9], and therefore, the role of gut microbiota and mixed infections should be studied further. The regulation of tight junction proteins is complex, including post-translational modifications. As such, these processes need to be studied in-depth to gain a comprehensive understanding of the role of malnutrition and tight junction proteins for intestinal barrier permeability [6,77]. Additionally, mucus production by goblet cells helps to prevent systemic dissemination of bacteria [78,79], but was not explored in this study. Indeed, a decrease in goblet cell number in both malnourished rats [80–82], pigs [83], and humans [84], as well as reduction in mucin content in animal models [80] and humans [85,86] has been described. We also did not investigate infiltration of immune cells nor those more specifically linked to IL22 secretion. Other elements of the inflammatory, metabolic and organ response, including cytokine profiles, serum albumin levels, blood glucose, and liver and kidney functions were also not examined, but have been shown to be altered in clinical and preclinical models of SM.

In summary, we demonstrated that LPD-fed mice exposed to DSS, or *C. rodentium* have a heightened disease susceptibility driven by an atypical colonic response to these insults compared to CPD-fed mice. These murine models provide valuable tools to investigate the pathophysiology of enteric infections in the context of malnutrition, especially in the colon where very little has been studied till date. Future research should leverage these models to identify and evaluate novel therapeutic agents that could be tested prior to being translated into clinical trials designed to improve long-term outcomes in children with severe malnutrition.

Supporting information

S1 Fig. Dose-dependent susceptibility of mice to DSS. (a) Schematic diagram for the mouse model of DSS-induced colitis; weanling C57Bl/6 mice fed control (CPD) or the low-protein diet (LPD) were treated with 2% DSS dissolved in drinking water for 5 days and DSS-free drinking water for the remainder of the 14-day experimental period. (b) Percent bodyweight change from day 0, (c) Clinical Severity Scoring (CSS) and (d) Survival was assessed. CSS is a measurement of hunched posture, ruffled fur, immobility, weight loss, diarrhea and bloody stools. Results are expressed as means ± SD and *p < 0.05; ***p < 0.001; ****p < 0.0001, as determined by (b-c) two-way ANOVA and mixed-effect analysis and (d) two-sided log-rank (Mantel-Cox).
(TIFF)

S2 Fig. Reductions in anthropometric measurements in low-protein fed mice post-infection with *C. rodentium*. (a) Tail length, (b) colon length, and (c) colon length normalized to tail length was measured at day 14 of the experimental period. (d) Viable *C. rodentium* counts in infected mice feces were quantified at day 7 post-infection in CPD and LPD mice. Results are expressed as means ± SD and *p < 0.05; ****p < 0.0001, as determined by (a-c) unpaired two tailed t-test analysis (n = 11/group), and (d) unpaired two tailed Mann-Whitney test (n = 11/group).
(TIFF)

S3 Fig. Uncropped western blots (a – gel 1, and b- gel 2) probed for OCCLUDIN, β-actin, and CLD-3 in colonic tissue of uninfected and infected CPD and LPD-fed mice.
(ZIP)

S1 Table. Composition of the model diets.
(DOCX)

S2 Table. Clinical Severity Scoring System to assess humane endpoints and minimize suffering to the animals.
(DOCX)

S3 Table. List of antibodies for Western Blot and IF.
(DOCX)

S1 File. Raw data.
(XLSX)

Acknowledgments

The authors thank the Imaging Facility at The Hospital for Sick Children for their technical help and support. We also want to thank Bernald Castro for technical support with histological staining. This work would not have been possible without Joel Tan (Dr. John Brumell lab), and Sharon Leung and Emiliano Miraglia (Dr. Peter Kim lab), who provided the wildtype strains of the bacterial pathogens and helped with the microbiology setup in the lab.

Author contributions

Conceptualization: Mehakpreet K. Thind, Mary Flanagan, Mishaal Munawar, Amber Farooqui, Celine Bourdon, Robert H. J. Bandsma.

Data curation: Mehakpreet K. Thind, Mary Flanagan, Sanne de Wit, Aida Glembocki, Jiali Pan, Celine Cuinat, Shamsun Nahar Shaima, Hamza Sghayare, Kinza Usmani, Amber Farooqui, Celine Bourdon, Robert H. J. Bandsma.

Formal analysis: Mehakpreet K. Thind, Mary Flanagan, Jiali Pan, Shamsun Nahar Shaima, Celine Bourdon, Robert H.J Bandsma.

Funding acquisition: Robert H. J. Bandsma.

Investigation: Mehakpreet K. Thind.

Methodology: Mehakpreet K. Thind, Mary Flanagan, Aida Glembocki, Jiali Pan, Celine Cuinat, Sharon Leung, Elena M. Comelli, Amber Farooqui, Celine Bourdon.

Project administration: Robert H. J. Bandsma.

Resources: Robert H. J. Bandsma.

Supervision: Robert H. J. Bandsma.

Writing – original draft: Mehakpreet K. Thind.

Writing – review & editing: Mehakpreet K. Thind, Mary Flanagan, Sanne de Wit, Aida Glembocki, Jiali Pan, Celine Cuinat, Sharon Leung, Peter Kim, Elena M. Comelli, Amber Farooqui, Celine Bourdon, Robert H. J. Bandsma.

References

1. Childhood Acute Illness and Nutrition (CHAIN) Network. Childhood mortality during and after acute illness in Africa and south Asia: a prospective cohort study. Lancet Glob Health. 2022;10(5):e673–84. https://doi.org/10.1016/S2214-109X(22)00118-8 PMID: 35427524
2. Bourke CD, Berkley JA, Prendergast AJ. Immune dysfunction as a cause and consequence of malnutrition. Trends Immunol. 2016. https://doi.org/10.1016/j.it.2016.04.003
3. Bhutta ZA, Berkley JA, Bandsma RHJ, Kerac M, Trehan I, Briend A. Severe childhood malnutrition. Nat Rev Dis Primers. 2017;3:17067. https://doi.org/10.1038/nrdp.2017.67 PMID: 28933421
4. Bourke CD, Jones KDJ, Prendergast AJ. Current understanding of innate immune cell dysfunction in childhood undernutrition. Front Immunol. 2019;10:1728. https://doi.org/10.3389/fimmu.2019.01728 PMID: 31417545
5. Maghraby MK, Li B, Chi L, Ling C, Benmoussa A, Provost P, et al. Extracellular vesicles isolated from milk can improve gut barrier dysfunction induced by malnutrition. Sci Rep. 2021;11(1):7635. https://doi.org/10.1038/s41598-021-86920-w PMID: 33828139
6. Ling C, Versloot CJ, Arvidsson Kvissberg ME, Hu G, Swain N, Horcas-Nieto JM, et al. Rebalancing of mitochondrial homeostasis through an NAD+-SIRT1 pathway preserves intestinal barrier function in severe malnutrition. EBioMedicine. 2023;96:104809. https://doi.org/10.1016/j.ebiom.2023.104809 PMID: 37738832
7. Amadi B, Besa E, Zyambo K, Kaonga P, Louis-Auguste J, Chandwe K, et al. Impaired barrier function and autoantibody generation in malnutrition enteropathy in Zambia. EBioMedicine. 2017;22:191–9. https://doi.org/10.1016/j.ebiom.2017.07.017 PMID: 28750860
8. Sturgeon JP, Njunge JM, Bourke CD, Gonzales GB, Robertson RC, Bwakura-Dangarembizi M, et al. Inflammation: the driver of poor outcomes among children with severe acute malnutrition? Nutr Rev. 2023;81(12):1636–52. https://doi.org/10.1093/nutrit/nuad030 PMID: 36977352
9. Attia S, Versloot CJ, Voskuijl W, van Vliet SJ, Di Giovanni V, Zhang L, et al. Mortality in children with complicated severe acute malnutrition is related to intestinal and systemic inflammation: an observational cohort study. Am J Clin Nutr. 2016;104(5):1441–9. https://doi.org/10.3945/ajcn.116.130518 PMID: 27655441
10. Wen B, Njunge JM, Bourdon C, Gonzales GB, Gichuki BM, Lee D, et al. Systemic inflammation and metabolic disturbances underlie inpatient mortality among ill children with severe malnutrition. Sci Adv. 2022;8(7):eabj6779. https://doi.org/10.1126/sciadv.abj6779 PMID: 35171682
11. Wen B, Farooqui A, Bourdon C, Tarafdar N, Ngari M, Chimwezi E, et al. Intestinal disturbances associated with mortality of children with complicated severe malnutrition. Commun Med (Lond). 2023;3(1):128. https://doi.org/10.1038/s43856-023-00355-0 PMID: 37773543
12. Njunge JM, Gwela A, Kibinge NK, Ngari M, Nyamako L, Nyatichi E, et al. Biomarkers of post-discharge mortality among children with complicated severe acute malnutrition. Sci Rep. 2019;9(1):5981. https://doi.org/10.1038/s41598-019-42436-y PMID: 30979939
13. Rytter MJH, Kolte L, Briend A, Friis H, Christensen VB. The immune system in children with malnutrition--a systematic review. PLoS One. 2014;9(8):e105017. https://doi.org/10.1371/journal.pone.0105017 PMID: 25153531

14. Phiri TN, Mutasa K, Rukobo S, Govha M, Mushayanembwa P, Mwakamui S, et al. Severe acute malnutrition promotes bacterial binding over proinflammatory cytokine secretion by circulating innate immune cells. Sci Adv. 2023;9(44):eadh2284. https://doi.org/10.1126/sciadv.adh2284 PMID: 37910623
15. Brown EM, Wlodarska M, Willing BP, Vonaesch P, Han J, Reynolds LA, et al. Diet and specific microbial exposure trigger features of environmental enteropathy in a novel murine model. Nat Commun. 2015;6:7806. https://doi.org/10.1038/ncomms8806 PMID: 26241678
16. Ibrahim MK, Zambruni M, Melby CL, Melby PC. Impact of childhood malnutrition on host defense and infection. Clin Microbiol Rev. 2017;30(4):919–71. https://doi.org/10.1128/CMR.00119-16 PMID: 28768707
17. Sturgeon JP, Mufukari W, Tome J, Dumbura C, Majo FD, Ngosa D. Risk factors for inpatient mortality among children with severe acute malnutrition in Zimbabwe and Zambia. Eur J Clin Nutr. 2023;77(9):895–904. https://doi.org/10.1038/s41430-023-01320-9
18. Weckman AM, McDonald CR, Ngai M, Richard-Greenblatt M, Leligdowicz A, Conroy AL, et al. Inflammatory profiles in febrile children with moderate and severe malnutrition presenting at-hospital in Uganda are associated with increased mortality. EBioMedicine. 2023;94:104721. https://doi.org/10.1016/j.ebiom.2023.104721 PMID: 37467665
19. Tickell KD, Sharmin R, Deichsel EL, Lamberti LM, Walson JL, Faruque ASG, et al. The effect of acute malnutrition on enteric pathogens, moderate-to-severe diarrhoea, and associated mortality in the Global Enteric Multicenter Study cohort: a post-hoc analysis. Lancet Glob Health. 2020;8(2):e215–24. https://doi.org/10.1016/S2214-109X(19)30498-X PMID: 31981554
20. Kebede F, Kebede T, Negese B, Abera A, Fentaw G, Kasaw A. Incidence and predictors of severe acute malnutrition mortality in children aged 6-59 months admitted at Pawe general hospital, Northwest Ethiopia. PLoS One. 2022;17(2):e0263236. https://doi.org/10.1371/journal.pone.0263236 PMID: 35213569
21. Salameh E, Morel FB, Zeilani M, Déchelotte P, Marion-Letellier R. Animal models of undernutrition and enteropathy as tools for assessment of nutritional intervention. Nutrients. 2019;11(9). https://doi.org/10.3390/nu11092233
22. Hidalgo-Villeda F, Million M, Defoort C, Vannier T, Svilar L, Lagier M, et al. Prolonged dysbiosis and altered immunity under nutritional intervention in a physiological mouse model of severe acute malnutrition. iScience. 2023;26(6):106910. https://doi.org/10.1016/j.isci.2023.106910 PMID: 37378323
23. Schwarzer M, Gautam UK, Makki K, Lambert A, Brabec T, Joly A, et al. Microbe-mediated intestinal NOD2 stimulation improves linear growth of undernourished infant mice. Science. 2023;379(6634):826–33. https://doi.org/10.1126/science.ade9767 PMID: 36821686
24. Schwarzer M, Makki K, Storelli G, Machuca-Gayet I, Srutkova D, Hermanova P, et al. *Lactobacillus plantarum* strain maintains growth of infant mice during chronic undernutrition. Science. 2016;351(6275):854–7. https://doi.org/10.1126/science.aad8588 PMID: 26912894
25. Hu G, Ling C, Chi L, Thind MK, Furse S, Koulman A, et al. The role of the tryptophan-NAD + pathway in a mouse model of severe malnutrition induced liver dysfunction. Nat Commun. 2022;13(1):7576. https://doi.org/10.1038/s41467-022-35317-y PMID: 36481684
26. Charbonneau MR, O'Donnell D, Blanton LV, Totten SM, Davis JCC, Barratt MJ, et al. Sialylated Milk oligosaccharides promote microbiota-dependent growth in models of infant undernutrition. Cell. 2016;164(5):859–71. https://doi.org/10.1016/j.cell.2016.01.024 PMID: 26898329
27. Littlejohn PT, Bar-Yoseph H, Edwards K, Li H, Ramirez-Contreras CY, Holani R, et al. Multiple micronutrient deficiencies alter energy metabolism in host and gut microbiome in an early-life murine model. Front Nutr. 2023;10:1151670. https://doi.org/10.3389/fnut.2023.1151670 PMID: 37497061
28. Littlejohn PT, Metcalfe-Roach A, Cardenas Poire E, Holani R, Bar-Yoseph H, Fan YM, et al. Multiple micronutrient deficiencies in early life cause multi-kingdom alterations in the gut microbiome and intrinsic antibiotic resistance genes in mice. Nat Microbiol. 2023;8(12):2392–405. https://doi.org/10.1038/s41564-023-01519-3 PMID: 37973864
29. Salameh E, Jarbeau M, Morel FB, Zeilani M, Aziz M, Déchelotte P, et al. Modeling undernutrition with enteropathy in mice. Sci Rep. 2020;10(1):15581. https://doi.org/10.1038/s41598-020-72705-0 PMID: 32973261
30. Wirtz S, Popp V, Kindermann M, Gerlach K, Weigmann B, Fichtner-Feigl S, et al. Chemically induced mouse models of acute and chronic intestinal inflammation. Nat Protoc. 2017;12(7):1295–309. https://doi.org/10.1038/nprot.2017.044 PMID: 28569761
31. Mullineaux-Sanders C, Sanchez-Garrido J, Hopkins EGD, Shenoy AR, Barry R, Frankel G. Citrobacter rodentium-host-microbiota interactions: immunity, bioenergetics and metabolism. Nat Rev Microbiol. 2019;17(11):701–15. https://doi.org/10.1038/s41579-019-0252-z PMID: 31541196
32. Hopkins EGD, Frankel G. Overview of the Effect of Citrobacter rodentium Infection on Host Metabolism and the Microbiota. In: Schüller S, Bielaszewska M, editors. Shiga Toxin-Producing E. coli: Methods and Protocols [Internet]. New York, NY: Springer US; 2021. pp. 399–418. https://doi.org/10.1007/978-1-0716-1339-9_20
33. Martin PK, Marchiando A, Xu R, Rudensky E, Yeung F, Schuster SL, et al. Autophagy proteins suppress protective type I interferon signalling in response to the murine gut microbiota. Nat Microbiol. 2018;3(10):1131–41. https://doi.org/10.1038/s41564-018-0229-0 PMID: 30202015
34. Conlin VS, Wu X, Nguyen C, Dai C, Vallance BA, Buchan AMJ, et al. Vasoactive intestinal peptide ameliorates intestinal barrier disruption associated with *Citrobacter rodentium*-induced colitis. Am J Physiol Gastrointest Liver Physiol. 2009;297(4):G735-50. https://doi.org/10.1152/ajpgi.90551.2008 PMID: 19661153
35. Koroleva EP, Halperin S, Gubernatorova EO, Macho-Fernandez E, Spencer CM, Tumanov AV. *Citrobacter rodentium*-induced colitis: a robust model to study mucosal immune responses in the gut. J Immunol Methods. 2015;421:61–72. https://doi.org/10.1016/j.jim.2015.02.003 PMID: 25702536
36. Brining DL, Mattoon JS, Kercher L, LaCasse RA, Safronetz D, Feldmann H, et al. Thoracic radiography as a refinement methodology for the study of H1N1 influenza in cynomologus macaques (Macaca fascicularis). Comp Med. 2010;60(5):389–95. PMID: 21262125

37. Sagaidak S, Taibi A, Wen B, Comelli EM. Development of a real-time PCR assay for quantification of *Citrobacter rodentium*. J Microbiol Methods. 2016;126:76–7. https://doi.org/10.1016/j.mimet.2016.05.008 PMID: 27196638

38. Erben U, Loddenkemper C, Doerfel K, Spieckermann S, Haller D, Heimesaat MM, et al. A guide to histomorphological evaluation of intestinal inflammation in mouse models. Int J Clin Exp Pathol. 2014;7(8):4557–76. PMID: 25197329

39. Schneider CA, Rasband WS, Eliceiri KW. NIH Image to ImageJ: 25 years of image analysis. Nat Methods. 2012;9(7):671–5. https://doi.org/10.1038/nmeth.2089 PMID: 22930834

40. Diaz LA, Altman NH, Khan WN, Serhan CN, Adkins B. Specialized proresolving mediators rescue infant mice from lethal *Citrobacter rodentium* infection and promote immunity against reinfection. Infect Immun. 2017;85(10):e00464–17. https://doi.org/10.1128/IAI.00464-17 PMID: 28694292

41. Wang S, Xia X, Liu Y, Wan F. Oral administration with live attenuated *Citrobacter rodentium* protects immunocompromised mice from lethal infection. Infect Immun. 2022;90(7):e0019822. https://doi.org/10.1128/iai.00198-22 PMID: 35861565

42. Bauer KC, York EM, Cirstea MS, Radisavljevic N, Petersen C, Huus KE, et al. Gut microbes shape microglia and cognitive function during malnutrition. Glia. 2022;70(5):820–41. https://doi.org/10.1002/glia.24139 PMID: 35019164

43. Shin AE, Tesfagiorgis Y, Larsen F, Derouet M, Zeng PYF, Good HJ, et al. F4/80+Ly6Chigh Macrophages Lead to cell plasticity and cancer initiation in colitis. Gastroenterology. 2023;164(4):593–609.e13. https://doi.org/10.1053/j.gastro.2023.01.002

44. Berger CN, Crepin VF, Roumeliotis TI, Wright JC, Serafini N, Pevsner-Fischer M, et al. The Citrobacter rodentium type III secretion system effector EspO affects mucosal damage repair and antimicrobial responses. PLoS Pathog. 2018;14(10):e1007406. https://doi.org/10.1371/journal.ppat.1007406 PMID: 30365535

45. Wen B, Taibi A, Villa CR, Lee S-H, Sagaidak S, Comelli EM. Effects of bifidobacterium bifidum in mice infected with *Citrobacter rodentium*. Microorganisms. 2019;7(2):51. https://doi.org/10.3390/microorganisms7020051 PMID: 30769786

46. Konturek PC, Harsch IA, Konturek K, Schink M, Konturek T, Neurath MF. Gut–liver axis: how do gut bacteria influence the liver? Med Sci. 2018;6(3):79. https://doi.org/10.3390/medsci6030079

47. Seki E, Schnabl B. Role of innate immunity and the microbiota in liver fibrosis: crosstalk between the liver and gut. J Physiol. 2012;590(3):447–58. https://doi.org/10.1113/jphysiol.2011.219691 PMID: 22124143

48. Lewis SM, Williams A, Eisenbarth SC. Structure and function of the immune system in the spleen. Sci Immunol. 2019;4(33):eaau6085. https://doi.org/10.1126/sciimmunol.aau6085 PMID: 30824527

49. Hashimoto T, Perlot T, Rehman A, Trichereau J, Ishiguro H, Paolino M, et al. ACE2 links amino acid malnutrition to microbial ecology and intestinal inflammation. Nature. 2012;487(7408):477–81. https://doi.org/10.1038/nature11228 PMID: 22837003

50. Walson JL, Berkley JA. The impact of malnutrition on childhood infections. Curr Opin Infect Dis. 2018;31(3):231–6. https://doi.org/10.1097/QCO.0000000000000448 PMID: 29570495

51. Tickell KD, Atlas HE, Walson JL. Environmental enteric dysfunction: a review of potential mechanisms, consequences and management strategies. BMC Med. 2019;17(1):181. https://doi.org/10.1186/s12916-019-1417-3 PMID: 31760941

52. Crane RJ, Jones KDJ, Berkley JA. Environmental enteric dysfunction: an overview. Food Nutr Bull. 2015;36(1 Suppl):S76–87. https://doi.org/10.1177/15648265150361S113 PMID: 25902619

53. Bein A, Fadel CW, Swenor B, Cao W, Powers RK, Camacho DM, et al. Nutritional deficiency in an intestine-on-a-chip recapitulates injury hallmarks associated with environmental enteric dysfunction. Nat Biomed Eng. 2022;6(11):1236–47. https://doi.org/10.1038/s41551-022-00899-x PMID: 35739419

54. Karunaratne R, Sturgeon JP, Patel R, Prendergast AJ. Predictors of inpatient mortality among children hospitalized for severe acute malnutrition: a systematic review and meta-analysis. Am J Clin Nutr. 2020;112(4):1069–79. https://doi.org/10.1093/ajcn/nqaa182 PMID: 32885807

55. Liu J, Ge X, Ouyang C, Wang D, Zhang X, Liang J, et al. Prevalence of malnutrition, its risk factors, and the use of nutrition support in patients with inflammatory Bowel disease. Inflamm Bowel Dis. 2022;28(Suppl 2):S59–66. https://doi.org/10.1093/ibd/izab345 PMID: 34984471

56. Rogawski ET, Liu J, Platts-Mills JA, Kabir F, Lertsethtakarn P, Siguas M, et al. Use of quantitative molecular diagnostic methods to investigate the effect of enteropathogen infections on linear growth in children in low-resource settings: longitudinal analysis of results from the MAL-ED cohort study. Lancet Glob Health. 2018;6(12):e1319–28. https://doi.org/10.1016/S2214-109X(18)30351-6 PMID: 30287125

57. Levine MM, Nasrin D, Acácio S, Bassat Q, Powell H, Tennant SM, et al. Diarrhoeal disease and subsequent risk of death in infants and children residing in low-income and middle-income countries: analysis of the GEMS case-control study and 12-month GEMS-1A follow-on study. Lancet Glob Health. 2020;8(2):e204–14. https://doi.org/10.1016/S2214-109X(19)30541-8 PMID: 31864916

58. Collins JW, Keeney KM, Crepin VF, Rathinam VAK, Fitzgerald KA, Finlay BB, et al. *Citrobacter rodentium*: infection, inflammation and the microbiota. Nat Rev Microbiol. 2014;12(9):612–23. https://doi.org/10.1038/nrmicro3315 PMID: 25088150

59. Yin Y, Wang R, Li Y, Qin W, Pan L, Yan C, et al. Protection against DSS-induced colitis in mice through FcεRIα deficiency: the role of altered Lactobacillus. NPJ Biofilms Microbiomes. 2024;10(1):84. https://doi.org/10.1038/s41522-024-00563-z PMID: 39266529

60. Hong D, Kim HK, Yang W, Yoon C, Kim M, Yang C-S, et al. Integrative analysis of single-cell RNA-seq and gut microbiome metabarcoding data elucidates macrophage dysfunction in mice with DSS-induced ulcerative colitis. Commun Biol. 2024;7(1):731. https://doi.org/10.1038/s42003-024-06409-w PMID: 38879692

61. Lopez CA, Miller BM, Rivera-Chávez F, Velazquez EM, Byndloss MX, Chávez-Arroyo A, et al. Virulence factors enhance *Citrobacter rodentium* expansion through aerobic respiration. Science. 2016;353(6305):1249–53. https://doi.org/10.1126/science.aag3042 PMID: 27634526

62. Patterson GT, Osorio EY, Peniche A, Dann SM, Cordova E, Preidis GA, et al. Pathologic inflammation in malnutrition is driven by proinflammatory intestinal microbiota, large intestine barrier dysfunction, and translocation of bacterial lipopolysaccharide. Front Immunol. 2022;13:846155. https://doi.org/10.3389/fimmu.2022.846155 PMID: 35720380

63. Lanyero B, Grenov B, Barungi NN, Namusoke H, Michaelsen KF, Mupere E, et al. Correlates of gut function in children hospitalized for severe acute malnutrition, a cross-sectional study in Uganda. J Pediatr Gastroenterol Nutr. 2019;69(3):292–8. https://doi.org/10.1097/MPG.0000000000002381 PMID: 31169661

64. Milatz S, Krug SM, Rosenthal R, Günzel D, Müller D, Schulzke J-D, et al. Claudin-3 acts as a sealing component of the tight junction for ions of either charge and uncharged solutes. Biochim Biophys Acta. 2010;1798(11):2048–57. https://doi.org/10.1016/j.bbamem.2010.07.014 PMID: 20655293

65. Assa A, Vong L, Pinnell LJ, Avitzur N, Johnson-Henry KC, Sherman PM. Vitamin D deficiency promotes epithelial barrier dysfunction and intestinal inflammation. J Infect Dis. 2014;210(8):1296–305. https://doi.org/10.1093/infdis/jiu235

66. Fine RL, Manfredo Vieira S, Gilmore MS, Kriegel MA. Mechanisms and consequences of gut commensal translocation in chronic diseases. Gut Microbes. 2020;11(2):217–30. https://doi.org/10.1080/19490976.2019.1629236 PMID: 31306081

67. Guttman JA, Finlay BB. Tight junctions as targets of infectious agents. Biochim Biophys Acta. 2009;1788(4):832–41. https://doi.org/10.1016/j.bbamem.2008.10.028 PMID: 19059200

68. Sharma D, Malik A, Guy CS, Karki R, Vogel P, Kanneganti TD. Pyrin inflammasome regulates tight junction integrity to restrict colitis and tumorigenesis. Gastroenterology. 2018;154(4):948–64.e8. https://doi.org/10.1053/j.gastro.2017.11.276

69. Thind MK, Miraglia E, Ling C, Khan MA, Glembocki A, Bourdon C, et al. Mitochondrial perturbations in low-protein-diet-fed mice are associated with altered neutrophil development and effector functions. Cell Rep. 2024;43(8):114493. https://doi.org/10.1016/j.celrep.2024.114493 PMID: 39028622

70. Holowka T, van Duin D, Bartelt LA. Impact of childhood malnutrition and intestinal microbiota on MDR infections. JAC Antimicrob Resist. 2023;5(2):dlad051. https://doi.org/10.1093/jacamr/dlad051 PMID: 37102119

71. Thind MK, Uhlig HH, Glogauer M, Palaniyar N, Bourdon C, Gwela A, et al. A metabolic perspective of the neutrophil life cycle: new avenues in immunometabolism. Front Immunol. 2024;14:1334205. https://doi.org/10.3389/fimmu.2023.1334205 PMID: 38259490

72. Melchior K, Gerner RR, Hossain S, Nuccio S-P, Moreira CG, Raffatellu M. IL-22-dependent responses and their role during *Citrobacter rodentium* infection. Infect Immun. 2024;92(5):e00099–24. https://doi.org/10.1128/iai.00099-24

73. Zheng Y, Valdez PA, Danilenko DM, Hu Y, Sa SM, Gong Q, et al. Interleukin-22 mediates early host defense against attaching and effacing bacterial pathogens. Nat Med. 2008;14(3):282–9. https://doi.org/10.1038/nm1720 PMID: 18264109

74. Yang W, Yu T, Huang X, Bilotta AJ, Xu L, Lu Y, et al. Intestinal microbiota-derived short-chain fatty acids regulation of immune cell IL-22 production and gut immunity. Nat Commun. 2020;11(1):4457. https://doi.org/10.1038/s41467-020-18262-6 PMID: 32901017

75. Nong H, Yuan H, Lin Y, Chen S, Li Y, Luo Z, et al. IL-22 promotes occludin expression by activating autophagy and treats ulcerative colitis. Mol Cell Biochem. 2023. https://doi.org/10.1007/s11010-023-04806-z

76. Shabgah AG, Navashenaq JG, Shabgah OG, Mohammadi H, Sahebkar A. Interleukin-22 in human inflammatory diseases and viral infections. Autoimmun Rev. 2017;16(12):1209–18. https://doi.org/10.1016/j.autrev.2017.10.004 PMID: 29037907

77. Chelakkot C, Ghim J, Ryu SH. Mechanisms regulating intestinal barrier integrity and its pathological implications. Exp Mol Med. 2018;50(8):1–9. https://doi.org/10.1038/s12276-018-0126-x

78. Metidji A, Omenetti S, Crotta S, Li Y, Nye E, Ross E, et al. The environmental sensor AHR protects from inflammatory damage by maintaining intestinal stem cell homeostasis and barrier integrity. Immunity. 2018;49(2):353–362.e5. https://doi.org/10.1016/j.immuni.2018.07.010 PMID: 30119997

79. Gustafsson JK, Navabi N, Rodriguez-Piñeiro AM, Alomran AHA, Premaratne P, Fernandez HR, et al. Dynamic changes in mucus thickness and ion secretion during *Citrobacter rodentium* infection and clearance. PLoS One. 2013;8(12):e84430. https://doi.org/10.1371/journal.pone.0084430 PMID: 24386378

80. Hill RB Jr, Prosper J, Hirschfield JS, Kern F Jr. Protein starvation and the small intestine. I. The growth and morphology of the small intestine in weanling rats. Exp Mol Pathol. 1968;8(1):66–74. https://doi.org/10.1016/0014-4800(68)90006-3 PMID: 5637108

81. Takano J. Intestinal changes in protein-deficient rats. Exp Mol Pathol. 1964;3:224–31. https://doi.org/10.1016/0014-4800(64)90055-3 PMID: 14194322

82. Vila CC, Saracino MP, Falduto GH, Calcagno MA, Venturiello SM, Pallaro AN, et al. Protein malnutrition impairs the immune control of Trichinella spiralis infection. Nutrition. 2019;60:161–9. https://doi.org/10.1016/j.nut.2018.10.024 PMID: 30599460

83. Neutra MR, Maner JH, Mayoral LG. Effects of protein-calorie malnutrition on the jejunal mucosa of tetracycline-treated pigs. Am J Clin Nutr. 1974;27(3):287–95. https://doi.org/10.1093/ajcn/27.3.287 PMID: 4205494

84. Kummerlowe C, Mwakamui S, Hughes TK, Mulugeta N, Mudenda V, Besa E, et al. Single-cell profiling of environmental enteropathy reveals signatures of epithelial remodeling and immune activation. Sci Transl Med. 2022;14(660):eabi8633. https://doi.org/10.1126/scitranslmed.abi8633 PMID: 36044598

85. Yu J, Ordiz MI, Stauber J, Shaikh N, Trehan I, Barnell E, et al. Environmental enteric dysfunction includes a broad spectrum of inflammatory responses and epithelial repair processes. Cell Mol Gastroenterol Hepatol. 2016;2(2):158–74.e1. https://doi.org/10.1016/j.jcmgh.2015.12.002

86. Kelly P, Amadi B, Chandwe K, Besa E, Zyambo K, Chama M, et al. Gene expression profiles compared in environmental and malnutrition enteropathy in Zambian children and adults. EBioMedicine. 2021;70:103509. https://doi.org/10.1016/j.ebiom.2021.103509 PMID: 34333236